BEST AVAILABLE IMAGES

Defective images within this document are accurate representations of the original documents submitted by the applicant.

Defects in the images may include (but are not limited to):

- BLACK BORDERS
- TEXT CUT OFF AT TOP, BOTTOM OR SIDES
- FADED TEXT
- ILLEGIBLE TEXT
- SKEWED/SLANTED IMAGES
- COLORED PHOTOS
- BLACK OR VERY BLACK AND WHITE DARK PHOTOS
- GRAY SCALE DOCUMENTS

IMAGES ARE BEST AVAILABLE COPY.

As rescanning documents *will not* correct images, please do not report the images to the Image Problem Mailbox.

Multiuser Detection for DS-CDMA UWB in the Home Environment

Qinghua Li, *Member, IEEE*, and Leslie A. Rusch, *Senior Member, IEEE*

Abstract—**We demonstrate the effectiveness of multiuser detection for an ultra-wideband (UWB) pulse based direct sequence spread spectrum system using code division multiple access. Extensive simulations were run using channel soundings of the 2–8 GHz band collected in a residential setting and characterized by a high level of multipath fragmentation. We show that the adaptive minimum mean square error (MMSE) multiuser detection (MUD) receivers are able to gather multipath energy and reject intersymbol and interchip interferernce for these channels to a much greater extent than RAKE receivers with 4 and 8 arms. We also demonstrate the adaptive MMSE is able to reject a narrowband IEEE 802.11a OFDM interferer, even for signal-to-interference ratio as severe as −30 dB. We show the adaptive MMSE exhibits only a 6 dB penalty relative to the single user case for the heavy multi-access interference (number of asynchronons users equal to spreading code length). The practical RAKE receivers were incapable of effectively rejecting either the strong narrowband interference or the heavily loaded wideband interference. Even more moderate levels of interference caused significant degradation in the performance of the practical RAKE receivers.**

I. Introduction

ULTRA-WIDEBAND (UWB) technology has attracted considerable interest in the research and standardization communities, due to its promising ability to provide high data rate at low cost with relatively low power consumption. As an overlay system, UWB will necessarily be required to operate in the presence of potentially strong and perhaps multiple interferers. Direct-sequence code-division multiple-access (DS-CDMA) is well-known as a powerful multiple-access technique in the presence of strong narrowband interference. While some examination of CDMA for UWB has been considered, it has mostly focused on time hopping and not direct sequence varieties, and dealt exclusively with treatment of wideband interference and not narrowband [1].

In this paper, we develop DS-CDMA receivers that combine the power of both UWB and DS-CDMA techniques. We propose adaptive multiuser receivers using minimum mean square error (MMSE) algorithms. These receivers are capable of combining energy from the dense multipath return of UWB systems [2]. The RAKE receiver is also very effective for multipath combining, however our simulations find that the MMSE are more effective than a four or eight fingered RAKE at multipath combining. RAKE receiver complexity goes up linearly for each path whose energy is exploited. The MMSE complexity is constant and always exploits all multipath energy present that falls in its observation window and is resolvable [2]. In addition, the MMSE has the advantage of suppressing intersymbol interference (ISI) due to paths within the observation window, which the RAKE receiver rejects only to the level of the processing gain.

While traditional matched filter and RAKE receivers can reject narrowband interference by exploiting the processing gain of the spread spectrum system, the MMSE multiuser detection (MUD) offers much greater interference rejection [3]. MUD is perhaps best known for its effectiveness in rejecting wideband interferers, or CDMA users in a network where simultaneous users access the channel using unique spreading codes [4]. Systems using carrier sense multiple access technique to access the channel are efficient when on average no more than one user is accessing the channel at any given time. CDMA systems are more efficient when there are many users, or when the duration of channel access is long [5]. For instance, for video delivery in home there may be only a handful of links active at any given time, but these are likely to be of extremely long duration. When all links are uncoordinated, CDMA can be an effective method of sharing the network under heavy load since collisions do not necessarily result in lost packets. CDMA systems on different overlay networks will reject the other networks in the same manner as interferers on the same network.

We test the MMSE MUD receivers in the presence of both narrowband IEEE 802.11a interference and co-channel UWB interference. Extensive simulations are presented using channel soundings of the 2–8 GHz band collected in a residential setting [10]. Simulation results demonstrate that the proposed receivers are capable of supporting up to 16 UWB users in 3–6 GHz band transmitting 100 Mb/s per user, using chip rates of 1.5 Gc/s with a signal-to-noise ratio (SNR) penalty of 4-6 dB over the more than single user channel. This same performance can also be achieved in the presence of a strong narrowband (NB) interferer. The conventional RAKE receiver technique shows high error floors in the presence of interference. The increased performance of the MMSE MUD receiver is achieved at the cost of high computational complexity.

In Section II, we describe the proposed DS-CDMA UWB system and the interference environment in which it will operate. We give the structure of the MMSE MUD receiver and RAKE receivers. In Section III, we develop analytical bit-error

Manuscript received December 14, 2001. This paper was presented in part at the IEEE Conference on Ultra-Wideband Systems and Technologies, 2002.

Q. Li is with Intel Labs, Intel Corporation, Santa Clara, CA 95052-8119 USA (e-mail: qinghua.li@intel.com).

L. A. Rusch is with the Department of Electrical and Computer Engineering, Université Laval, QC GIK 7P4, Canada (e-mail: rusch@gel.ulaval.ca).

Digital Object Identifier 10.1109/JSAC.2002.805241

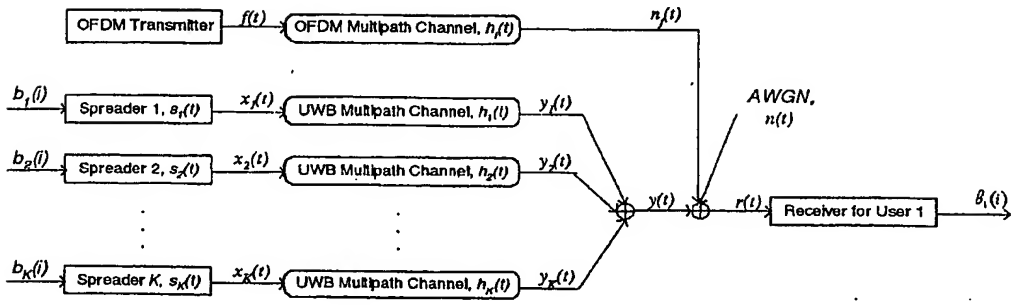

Fig. 1. System model.

rate (BER) expressions for the receivers under the simplifying assumptions of equal power CDMA users and approximate Gaussian distribution of the interferers. In Section IV, we present results from our extensive simulations using multipath data gathered for 2–8 GHz in a residential environment, summarizing our results in Section V.

II. System Description

We consider a K-user DS-CDMA system signaling through multipath UWB channels, where each user employs binary phase-shift keying (BPSK) direct-sequence spread-spectrum (DSSS) modulation. We consider the problem of detecting one desired user's bits. The block diagram of the system is illustrated in Fig. 1.

A. Transmitter Structure

The transmitter end is shown in the upper left part of Fig. 1. The equiprobable binary bit stream $\{b_k(i)\} \in \{1,-1\}_{i=1}^{M}$ for user $k, k = 1,\ldots,K$, is BPSK modulated by a signature waveform $s_k(t)$. That is, $b_k(i) = 1$ is mapped to $s_k(t)$ and $b_k(i) = -1$ is mapped to $-s_k(t)$. M is the number of bits per packet and there are K simultaneous, asynchronous DS-CDMA users. Each DSSS signal is then transmitted through its multipath channel $h_i(t)$. The transmitted signal generated by the kth user is given by

$$x_k(t) = \sum_{i=1}^{M} b_k(i) \cdot s_k(t). \tag{1}$$

The bit $b_k(i)$ could be either a data bit or a training bit that is known to receivers. It is assumed that $s_k(t)$ has unit energy and consists of N UWB pulses that are modulated by the signature sequence of user k. For this analysis and simulation, we make the simplifying assumption that all users are received with equal power.

In this model, the UWB pulse denoted by $p(t)$ is assumed to include the differential effects in the transmitter and receiver antenna systems. A typical pulse employed in the literature [1], [6] is the second derivative of a Gaussian pulse given by

$$p_2(t) = \left[1 - 4\pi\left(\frac{t}{\tau_m}\right)\right]\exp\left[-2\pi\left(\frac{t}{\tau_m}\right)^2\right]. \tag{2}$$

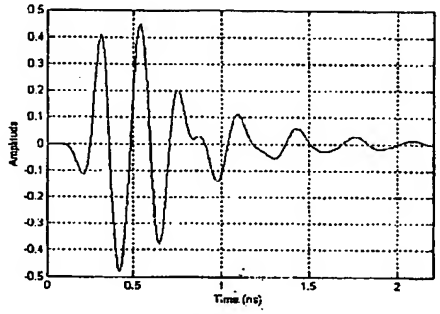

Fig. 2. The pulse shape after bandpass filtering.

Due to the anticipated Federal Communication Committee (FCC) restrictions on UWB overlay, we employ bandpass filtering to the transmitted pulse. The pulse $p_2(t)$ after the bandpass filter is depicted in Fig. 2.

B. Channel Model

We assume a time-invariant, asynchronous multipath channel for each user. The kth user's signal is transmitted through the multipath channel with impulse response (IR) $h_k(t)$. The received signal due to user k is

$$y_k(t) = x_k(t) \otimes h_k(t) \tag{3}$$

where $\otimes$ denotes convolution. The total received signal is then

$$r(t) = \sum_{k=1}^{K} y_k(t) + n_f(t) + n(t) \tag{4}$$

where $n_f(t)$ is a zero-mean narrowband OFDM signal corrupted by multipath fading, and $n(t)$ is zero-mean additive white Gaussian noise (AWGN). Although not shown explicitly in (3), we assume random time delays in channel IRs $h_k(t)$ for the asynchronous case.

C. Receiver Structure

The MMSE receiver consists of a bandpass filter and an adaptive filter. The bandpass filter suppresses noise and interference out of signal band to increase SNR. The adaptive filter is a finite-impulse response (FIR) filter that essentially acts as a

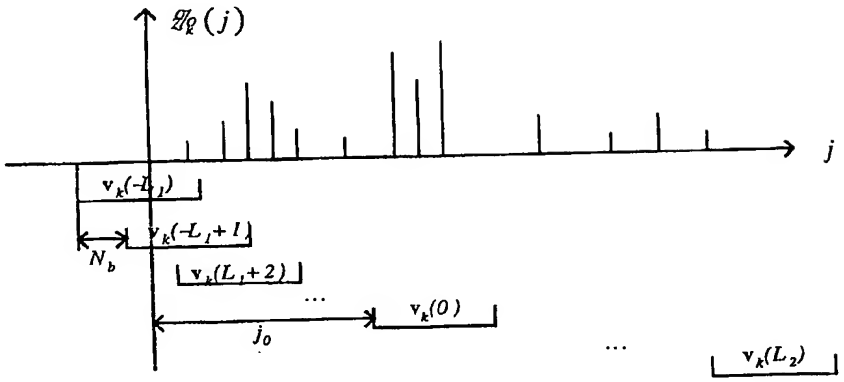

Fig. 3. Illustration of $\mathbf{v}_k(l)$.

correlator. While a matched filter correlates with the transmitted waveform, the MMSE is the linear filter that minimizes the MSE no matter what type of noise may be present.

At each bit epoch, a bit decision is made at the output of correlator and is then fed back to the adaptive filter. The observation window of the filter is typically longer than 1 bit interval and, therefore, windows overlap in time. Tap weights for the adaptive filter are adjusted adaptively using least mean square (LMS) or recursive least squares (RLS) [7]. The adaptation works in two stages (training and decision directed), initially using a training sequence to adapt to the channel, and then in decision directed mode using hard decisions at the correlator output. A summary of the discrete time MMSE algorithms is given in the Appendix, with notation defined in Section III.

III. Performance Analysis

The BER performance of the MMSE receiver is derived in this section. We assume without loss of generality that user 1 is the desired user.

A. Performance of MMSE Receiver

Let the observation window of the MMSE filter be of duration $_w$. The ith window is given by

$$(t_0 + (i-1)T_b, t_0 + (i-1\ T_b + T_w)$$

where $_b \triangleq$ 1/symbol rate. We set t_0 so that the ith observation window contains the bulk of the energy from user 1's ith bit (in the simulations we use side information about the channel, in a practical receiver an autocorrelation peak could be used to detect crude timing information).

For notational simplicity, we employ a discrete time model. The received signal (t) in (4) is first filtered by a bandpass filter to suppress out-of-band noise, assisting convergence of the adaptive filter. Denote the bandpass filter output as $r_b(t)$, which is sampled at a rate f_s greater than the Nyquist rate. Suppose user k transmits a single positive bit through the channel which is received as

$$z_k(t) = s_k(t) \otimes h_k(t) \otimes h_b(t), \quad k = 1, \ ,\ldots, K \qquad (5)$$

where $h_b(t)$ is the IR of the bandpass filter. Define L_1 and L_2 such that any of the multipath corrupted signals, $\{z_k(t)\}_k^K$, is limited to $L_1 + L_2 + 1$ observation windows

$$(t_0 + (i- \ )T_b, t_0 + (i-1)T_b + T_w), i = -L_1, -L_1+1\ \ldots, L_2.$$

That is, when detecting the first bit of user 1, observation windows $-L_1$ to L_2 will contain all energy from user k for that single bit. Define

$$T_s \triangleq \frac{1}{f_s}; \quad N_b \triangleq \frac{T_b}{T_s}; \quad _w \triangleq \frac{T_w}{T_s}; \quad j_0 \triangleq \frac{t_0}{T_s} \qquad (6)$$

$$\tilde{z}_k\ j) \triangleq z_k(j\ _s), \quad \tilde{r}(j) \triangleq r\ (jT_s), \quad \tilde{n}_f(\ ) \triangleq n_{fb}(jT_s)$$
$$\tilde{n}(j) \triangleq n_b(jT_s) \qquad (7)$$

for $j = 1, 2, \ldots$ and where N_b, N_w, and j_0 are assumed to be integers; N_w is the number of samples in each observation window; the symbols with a tilde denote the corresponding discrete time samples of the continuous time signals previously defined; $r_b(\cdot), n_{fb}(\cdot)$, and $n_b(\cdot)$ denote the bandpass filtered versions of $r(\cdot), n_f(\cdot), n(\cdot)$, respectively. We will now parse the signal $\tilde{z}_k(j)$ into overlapping segments that represent its contribution to each observation window that it affects. The segmentation is

$$\mathbf{v}_k(l \triangleq [\tilde{z}_k(i_0 + lN_b + 1) \quad \tilde{z}_k(i_0 + lN_b + 2)$$
$$\cdots \quad \tilde{z}_k(i_0 + l\ _b + N_w)]^T, \quad l = -L_1, \ldots, L_2 \qquad (8)$$

where $\tilde{z}_k(j) = 0$ outside the finite IR of the channel. Fig. 3 illustrates the segmentation of $\tilde{z}_k(j)$ into overlapping segments $v_k(l)$. Recall that the ith bit decision for user 1 occurs in window i.

Denote the adaptive filter taps and the received signal in the ith bit's observation window, respectively, as

$$\mathbf{w} \triangleq [w(1) \quad w(2) \quad \cdots \quad w(N_w)]^T; \qquad (9)$$

$$\mathbf{u}(i) \triangleq [\tilde{r}(i_0 + (i-1)N_b + 1) \quad \tilde{r}(j_0 + (i-1)N_b + 2)$$
$$\cdots \quad \tilde{r}(j_0 + (i-1)N_b + N_w)]^T. \qquad (10)$$

Now using (7), we rewrite (10) as

$$\mathbf{u}(i) = \sum_{k=1}^{K} \sum_{l=-L_1}^{L_2} b_k(i-l)\mathbf{v}_k(l) + \mathbf{n}_f(i) + \mathbf{n}(i) \quad \text{for } L_2 < i \tag{11}$$

where the sampled versions of the NB interferer and AWGN are given, respectively, as

$$\mathbf{n}_f \triangleq [\tilde{n}_f(j_0 + (i-1)N_b + 1) \quad \tilde{n}_f(j_0 + (i-1)N_b + 2) \quad \cdots \quad \tilde{n}_f(j_0 + (i-1)N_b + N_w)]^T \tag{12}$$

$$\mathbf{n} \triangleq [\tilde{n}(j_0 + (i-1)N_b + 1) \quad \tilde{n}(j_0 + (i-1)N_b + 2) \quad \cdots \quad \tilde{n}(j_0 + (i-1)N_b + N_w)]^T. \tag{13}$$

The optimal MMSE filter taps $\tilde{\mathbf{w}}$ to detect user 1's ith bit are given by

$$\begin{aligned}\tilde{\mathbf{w}} &= \arg \min_{\mathbf{w} \in \mathbb{C}^{N_w}} E\{\|b_1(i) - \mathbf{w}^H \mathbf{u}(i)\|^2\} \\ &= \arg \min_{\mathbf{w} \in \mathbb{C}^{N_w}} \mathbf{w}^H E\{\mathbf{u}(i)\mathbf{u}^H(i)\}\mathbf{w} \\ &\quad - 2\mathrm{Re}\{\mathbf{w}^H E\{b_1(i)\mathbf{u}(i)\}\}\end{aligned} \tag{14}$$

where ^{H} denotes conjugate transpose.

We assume independence between all users' bits $b_k(i)$, interference $n_f(i)$, and noise $n(i)$. From (14) and the independence, the two expectations in (14) are given by

$$E\{\mathbf{u}(i)\mathbf{u}^H(i)\} = \sum_{k=1}^{K} \sum_{l=-L_1}^{L_2} \mathbf{v}_k(l)\mathbf{v}_k^H(l) + \mathbf{R}_f + \mathbf{R} \tag{15}$$

$$E\{b_1(i)\mathbf{u}(i)\} = \mathbf{v}_1(0) \tag{16}$$

where $\mathbf{R}_f \triangleq E\{\mathbf{n}_f\mathbf{n}_f^H\}$ and $\mathbf{R} \triangleq E\{\mathbf{n}\mathbf{n}^H\}$. The solution to (14) is then given by

$$\tilde{\mathbf{w}} = \left[\sum_{k=1}^{K} \sum_{l=-L_1}^{L_2} \mathbf{v}_k(l)\mathbf{v}_k^H(l) + \mathbf{R}_f + \mathbf{R}\right]^{-1} \mathbf{v}_1(0). \tag{17}$$

The matrix $\mathbf{R}_f$ and $\mathbf{R}$ are the covariance matrixes of $\mathbf{n}_f$ and $\mathbf{n}$, which consist of autocorrelation coefficients of lags of $\tilde{n}_f(j)$ and $\tilde{n}(j)$. Since $n(t)$ is AWGN and the response of the receiver's bandpass filter is known, the autocorrelation function of $\tilde{n}(j)$ can be computed, leading to the matrix $\mathbf{R}$. Note that $n_f(t)$ is a narrowband multipath-corrupted OFDM signal. $\mathbf{R}_f$ can be computed from the spectrum or the autocorrelation function of $n_f(t)$.

Before computing the BER of the optimal MMSE receiver, we derive the distributions of the three residual impediments at the output of the adaptive filter: 1) AWGN; 2) multiaccess interference (MAI); and 3) OFDM interferer. Denote the ith output of the MMSE filter as

$$\beta(i) \triangleq \tilde{\mathbf{w}}^H \mathbf{u}(i) = \tilde{\mathbf{w}}^H \mathbf{v}(0) b_1(i) + e_m(i) + e_f(i) + e_g(i) \tag{18}$$

where $e_m(i)$ is the residual MAI; $e_f(i)$ is the residual OFDM interference; and $e_g(i)$ is the residual Gaussian noise, all after filtering. Due to assumptions made in Section II, $e_m(i)$, $e_f(i)$, and $e_g(i)$ have zero mean. Both the bandpass and MMSE filtering are linear operations, therefore, $e_g(i)$ is a linear combination of Gaussian noise $n(t)$, and $e_g(i)$ is Gaussian. In [8], it is shown that the distribution of the MAI at the output of a linear MMSE multiuser receiver is approximately Gaussian under general conditions. Next, we show $e_f(i)$ is approximately Gaussian.

Denote the signal at the output of OFDM transmitter as $f(t)$ as shown in Fig. 1. Then, $f(l)$ is given by

$$f(l) = \sum_{m=1}^{\Omega} g_m(t) \tag{19}$$

where Ω is the number of subcarriers and $g_m(t)$ is the modulated signal on the mth subcarrier. For random data $g_m(t)$ are independent of each other for $m = 1, \ldots \Omega$. The magnitude of $g_m(t)$ is bounded, i.e., $|g_m(t)| < A$, and we assume each subcarrier has the same power, i.e., $\mathrm{Var}\{g_m(t)\} = P_0$. By a corollary of central limit theorem [9], $n_f(t)$ is asymptotically Gaussian for large Ω. For instance, IEEE 802.11a systems meet these assumption and have Ω large (52 subcarriers). Since multipath channel $h_f(t)$, bandpass filter, and the MMSE filter are all linear operaters, $e_f(i)$ is a linear combination of $f(t)$ and, thus, it is approximately Gaussian.

Since the noise terms in (18), $e_m(i), e_f(i)$, and $e_g(i)$ are independent and approximately zero mean and Gaussian, the BER is given by

$$P_e = Q\left(\sqrt{\frac{\tilde{\mathbf{w}}^H \mathbf{v}_1(0)}{\sigma_m^2 + \sigma_g^2 + \sigma_f^2}}\right) \tag{20}$$

where σ_m^2, σ_g^2, and σ_f^2 are the variances of $e_m(i), e_f(i)$, and $e_g(i)$, respectively. The variances are given by

$$\sigma_m^2 = \sum_{k=2}^{K} \sum_{l \neq 0} |\tilde{\mathbf{w}}^H \mathbf{v}_k(l)|^2 \tag{21}$$

$$\sigma_g^2 = \sigma^2 \sum_j |h_{bw}(j)|^2 \tag{22}$$

where $h_{bw}(j) \triangleq h_b(j) \otimes \tilde{w}(j)$ is the combined equivalent filter response of the receiver bandpass filter and the optimal adaptive filter $\tilde{\mathbf{w}}$; $2\sigma^2$ is the power spectral density of the AWGN; σ_f^2 is determined by the spectrum of $n_f(t)$ and the filter $h_{bw}(j)$. Once the system parameters are known, i.e., UWB users' spreading waveforms, OFDM interferer's constellation, and the multipath channels, the BER can be computed.

The ideal MMSE tap weights are computed for each of the channel realizations in the simulation section, using information on the bandpass filter, OFDM spectrum, etc. The BER performance of these receivers is averaged and presented in the curves labeled "MMSE analytic." They represent a lower bound on the performance of the adaptive versions of the MMSE receiver.

B. Performance of RAKE Receiver

We compute the optimal performance of the RAKE receiver next. To achieve the optimal performance, we assume the receiver knows the desired user's channel IR and there are an infinite number of fingers available. Under these assumptions, the optimal RAKE receiver can be implemented as a matched filter matched to the desired user's received signal, $y_1(l)$, shown in Fig. 1.

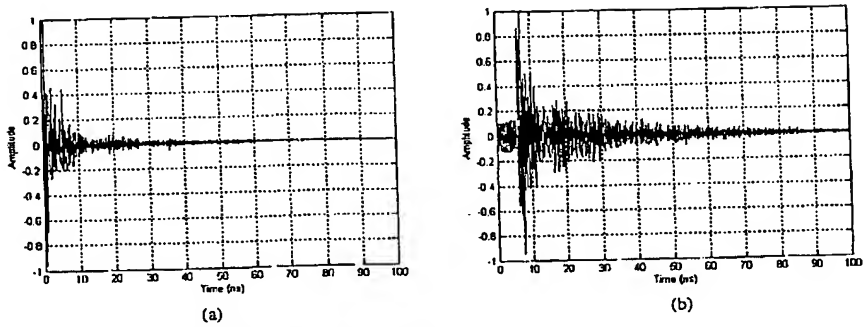

Fig. 4. A measured UWB channel IR (a) line-of-sight and (b) nonline-of-sight.

We employ the same discrete time model and notations in Section III to find the filter taps w matched to $y_1(t)$. Using the previous development for the MMSE filter, we can find the ideal RAKE receiver by the following manipulations: 1) set the IR of the receiver bandpass filter to the Dirac delta function, i.e., $h_b(t) = \delta(t)$ (as the RAKE receiver does not need the bandpass filter); 2) set the window delay j_0 to zero; 3) set the observation window width to the duration of user 1's received symbol length, i.e., the length of $z_1(t)$ in (5); and 4) set the filter weights w to

$$\tilde{\mathbf{w}} = [y_1(T_s) \quad y_1(2T_s) \quad \cdots \quad y_1(N_w T_s)] \tag{23}$$

To find the BER performance, we must further assume that the MAI is Gaussian. This is a reasonable assumption for large numbers of users with similar received powers, i.e., the receiver does not encounter near–far problem. By substituting the filter tap weights of (17) with those of (23), the BER of the optimal RAKE receiver is given by (20)–(22). The optimal RAKE is computed for each of the channel realizations in the simulation section. Since the performance tracks with that of the infinite RAKE simulations they are not reported in the figures.

IV. Simulation Results

In this section, we present extensive simulation results for the performance of a DS-CDMA system with three types of receivers: 1) the matched filter receiver; 2) the RAKE receiver; and 3) the MMSE receiver. We use a chip rate of 1.5 GHz and length 15 spreading code (Kasami codes were used). All simulations use the multipath UWB channels that are randomly selected from 800 UWB channel realizations measured in a home environment as reported in [10]. Our goal is to examine the performance for the following scenarios:

a) multipath channel, no interferers;
b) multipath channel, one NB interferer;
c) multipath channel, multiple DS-CDMA UWB signals;
d) multipath channel, one NB interferer and multiple DS-CDMA UWB signals.

The receivers will do well in scenario (a) if they can capture a large percentage of the multipath energy, while combating intersymbol and interchip interference (ISI). In scenarios (b), (c), and (d), the receivers must suppress differing sources of interference, as well as providing multipath combining and reducing ISI.

Due to space constraints the majority of results presented are for the more realistic and challenging nonline-of-sight (NLOS) channel. We have completed line-of-sight (LOS) simulations as well and report these results qualitatively in the text. Simulations represent the BER after averaging over 20 or 50 channels. Twenty channels were used instead of 50, when simulation time was excessive, i.e., where we vary the SNR, as well as the signal-to-interference ratio (SIR); SNR $\triangleq (E_b/N_0)$ and SIR $\triangleq$ (Power of UWB/Power of OFDM). Note that SNR and SIR values are as measured at the receiver and, therefore we examine the multipath performance, but not the fading performance.

The channel impulses employed in analysis and simulation are measured in an indoor environment, inside a townhouse [10]. One "typical" LOS and one "typical" NLOS channel IR are shown in Fig. 4. The channel IRs in the 2–8-GHz band were sampled at 16 GHz. We used an order 6 Chebyshev bandpass filter at both transmitter and receiver, with passband 3–6 GHz for all simulations. Simulations were completed with the 16 GHz sampling rate.

The narrowband interference we generate is an IEEE 802.11a OFDM signal that occupies a relatively narrowbandwidth compared with that of UWB. This interferer was chosen, as the frequency range for a UWB overlay system is likely to include the 5 GHz band where the IEEE 802.11a system operates. The popularity of IEEE 802.11b wireless local area networks presages the possible extensive use of the higher bit rate 802.11a systems. In our simulations, the OFDM signal passes through one of the typical UWB channels measured in [10]. We vary the received SIR for the OFDM system from -30 to 0 dB relative to the received signal energy of the desired UWB signal. This interference range was selected based on the following discussion. Assuming the UWB system has a 3-GHz bandwidth and was allowed to operate at FCC part 15 signal levels of -41 dBm per MHz, and also assuming the OFDM signal was transmitted 100 mW, the SIR would be -26 dB for the UWB and OFDM transmitters equally distant from the UWB receiver. The 0 dB value of SIR corresponds roughly to an OFDM transmitter some 5 m more distant than the UWB transmitter.

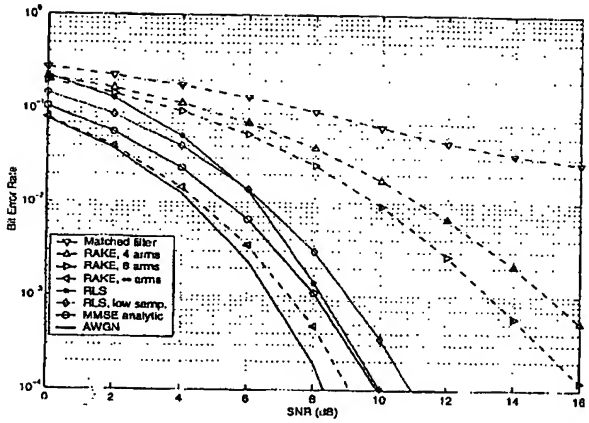

Fig. 5. BER performance in single-user NLOS UWB channels without interference.

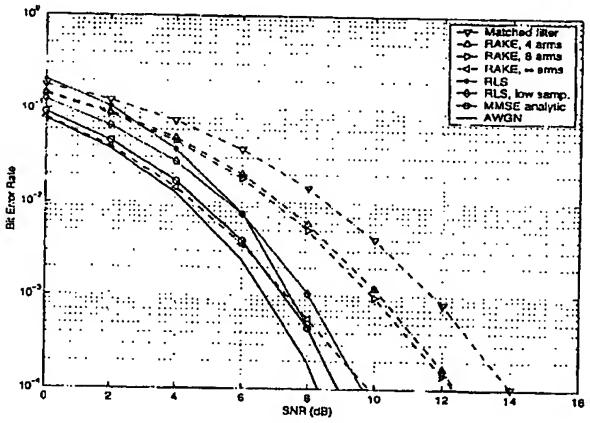

Fig. 6. BER performance in single-user LOS UWB channels without interference.

The wideband interference is the MAI from other UWB users operating in a DS-CDMA network. We only examine the situation where all interfering UWB signals arrive at the receiver with equal energies. We present results for 0 to 15 such interferers, which gives a simplistic indication of performance in the presence of stronger interferers (i.e., 15 equal power interferers could be compared with a single user that is 12 dB stronger).

The RAKE receivers implemented include the matched filter or single finger RAKE, a four finger, an eight finger, and an infinite finger RAKE. Side information of channels is used to perform maximum ratio combining [11] for all RAKE receivers. The infinite RAKE (actually about 1200 fingers depending on channel realization) uses exact information about the channel to essentially capture all multipath energy and is not practically implementable, but is included as a bound to RAKE performance. We restrict the multiple finger RAKE receivers to have minimum 250 ps time separation between fingers as a reasonable physical limitation for receiver hardware. Moreover, the fingers are located at the time delays that correspond to the greatest peaks of matched filter output with only one symbol transmitted.

The MMSE multiuser detector is implemented adaptively using both the RLS and LMS adaptive algorithms. We use training signals of 500 bits followed by decision directed operation. With the channel unchanged, we average over many packets to measure the BER, using decision directed mode exclusively in noninitial packets and allowing the adaptation to continue from its previous settings. We will see that the RLS receiver is more robust to differing interferers, indeed the LMS is unable to reject strong (SIR $= -30$ dB) narrowband interference. Two versions of these adaptive receivers are presented: 1) a high-order filter (tap spacing of 62.5 ps) that could represent an infinite tap MMSE, or an analog MMSE; and 2) a more realistic lower sample rate version that has tap spacing equal to half a chip interval, or 333 ps. The observation window of the MMSE detector is taken to be two symbols

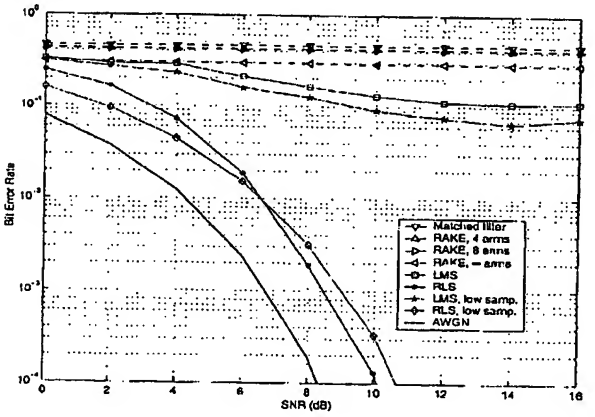

Fig. 7. BER performance in single-user NLOS UWB channels with OFDM interference. $\hbox{SIR} = -30$ dB.

(60 samples for low sampling rate version). We use side information about the channel to center the early paths in the front one third of the observation window. (Without side information the autocorrelation peak could give crude timing information for this placement.) All CDMA users operate asynchronously and no timing recovery is needed by the adaptive MMSE receiver.

Simulations results are presented in the ensuing sections. Section IV-A covers scenario (a) of a multipath channel with no interference and serves as baseline performance of the receivers under examination. Section IV-B examines performance for scenario (b) where one OFDM 802.11a NB interferer is present. Section IV-C examines scenario (c), a CDMA system with up to 16 simultaneous users accessing the same bandwidth (wideband interference). Finally, Section IV-D covers scenario (4) where both narrowband and wideband interference is present.

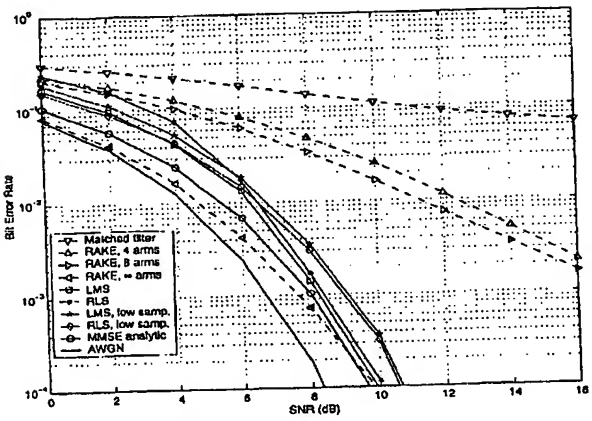

Fig. 8. BER performance in single-user NLOS UWB channels with OFDM interference. $hbox{SIR} = 0$ dB.

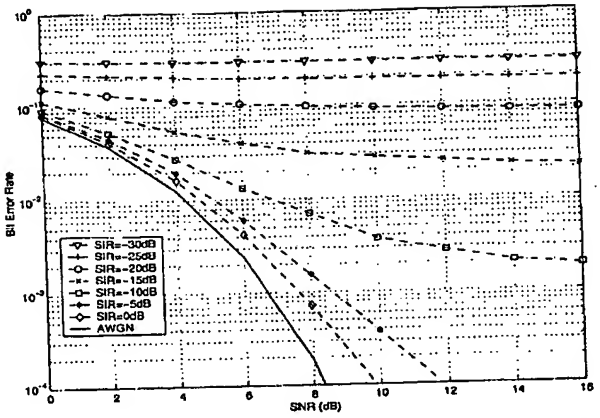

Fig. 10. The BER performance of infinite finger RAKE receiver for a single UWB user in NLOS UWB channels and in the presence of one OFDM interferer. SIR varies from −30 to 0 dB with 5 dB increment.

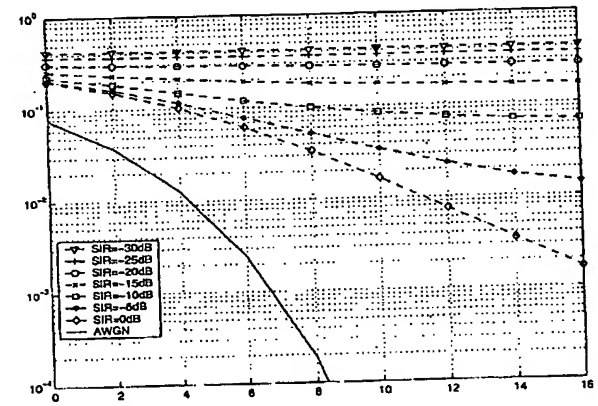

Fig. 9. The BER performance of eight finger RAKE receiver for a single UWB user in NLOS UWB channels and in the presence of one OFDM interferer. SIR varies from −30 to 0 dB with 5 dB increment.

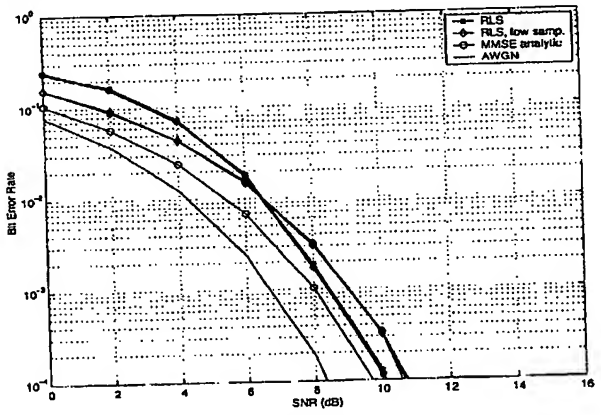

Fig. 11. The BER performance of MMSE receivers using RLS algorithm with Nyquist sampling rate and less for a single UWB user in NLOS UWB channels and in the presence of one OFDM interferer. SIR varies from −30 to 0 dB with 5 dB increment.

A. Multipath Channel, No Interferers

Results for this section are presented in Fig. 5 for NLOS and Fig. 6 for LOS, where we have averaged over 50 UWB channels in each case. The curves marked AWGN are the performance of maximum-likelihood (ML) receiver in an AWGN single path channel. The infinite RAKE is an idealized receiver that achieves within 1 dB of the AWGN bound, suffering only slightly from ISI due to the high processing gain of this receiver. The matched filter or single finger RAKE is a poor performer, while the 4- and 8-finger RAKEs are able to capitalize on the multipath energy to a limited extent. The MMSE analytic curve is calculated using (14) with zero interfering energy; it represents the best possible performance of the adaptive MMSE and has a 1 dB penalty relative to the infinite RAKE. The adaptive versions with high sampling rate show almost ideal performance for high SNR, but a 1 dB penalty at low SNR due to errors in the decision directed mode. The lower sampling rate adaptive MMSE exhibits only a 1 dB penalty relative to the analytic MMSE results. Although curves are only presented for the RLS version (due to space constraints), results for the LMS are almost identical.

Comparing Figs. 5 to 6, we see that the LOS channels lead to better performance for the matched filter and 4- and 8-finger RAKEs. This is due to the LOS channels packing more energy into fewer paths, giving a 3–6 dB-advantage relative to NLOS. The MMSE detectors also benefit by approximately 1 dB from a tighter packing of multipath energy (lower mean excess delay), as more of the multipath energy is contained in the observation interval. The AWGN and infinite RAKE results are unchanged as they already gather all energy. No other results are presented for LOS channels due to space constraints, however, comparable qualitative results for the relative performance of receivers in LOS and NLOS hold through for all scenarios. Note

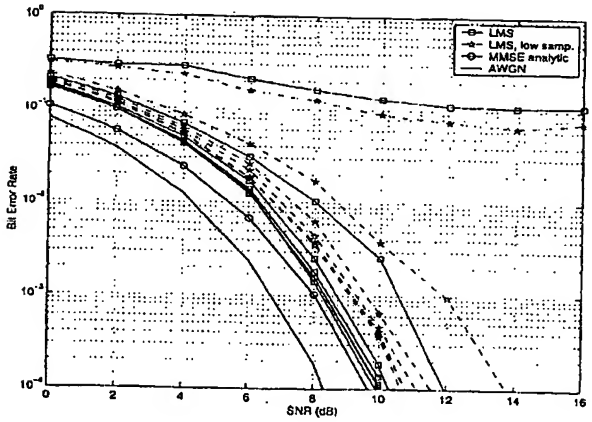

Fig. 12. The BER performance of MMSE receivers using LMS algorithm with Nyquist sampling rate and less for a single UWB user in NLOS UWB channels and in the presence of one OFDM interferer. SIR varies from −30 to 0 dB with 5 dB increment.

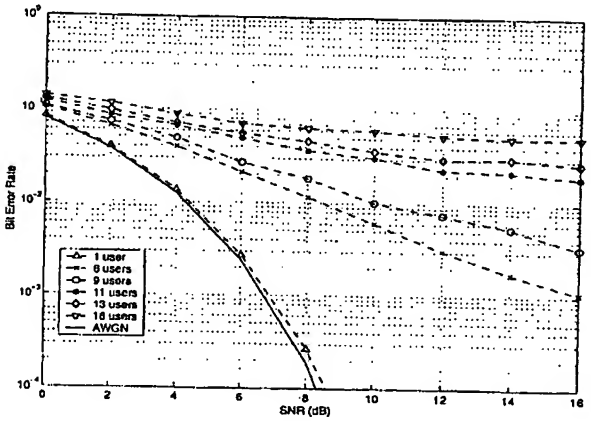

Fig. 14. BER performance of the infinite finger RAKE. The desired user's channel is fixed on a NLOS UWB channel [see Fig. 4(b)]. The number of UWB users varies from 1 to 16, where all users have the same received power.

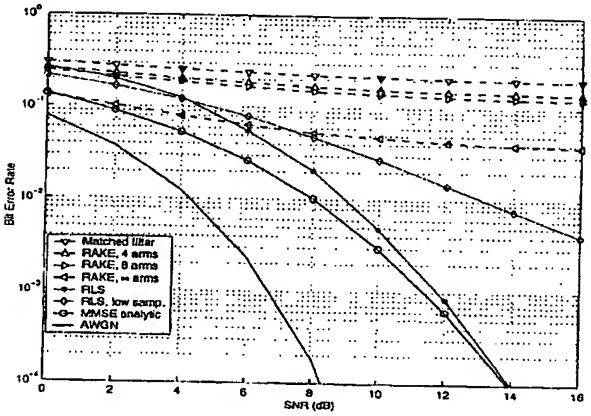

Fig. 13. The BER performance in NLOS UWB channels in the presence of 15 UWB interferers all with the same received power.

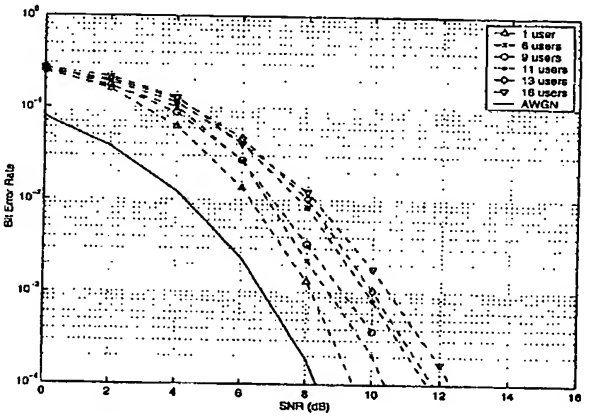

Fig. 15. BER performance of MMSE receiver using RLS algorithm. The desired user's channel is fixed on a NLOS UWB channel [see Fig. 4(b)]. The number of UWB users varies from 1 to 16, where all users have the same received power.

that the MMSE receiver exploits only the signal in the observation window, i.e., a segmentation of 20 ns, whereas the infinite RAKE receiver operates on the whole received spread symbol.

B. Multipath Channel, One NB Interferer

Results for this section are presented in Figs. 7–12, where we have averaged over 20 UWB sets of channels in each case. The SIR is varied from 0 dB (i.e., equal received energy for UWB and interferer) to −30 dB (interferer 30-dB stronger than the UWB signal). Roughly speaking, 0 dB SIR corresponds to the interferer being 5 m more distant that the desired UWB transmitter, while −26 dB is for equidistant transmitters. First, the extreme values of SIR are plotted to see general receiver performance, then, specific receivers are shown for the entire range of SIR values.

In Fig. 7, we see the matched filter, 4 and 8 finger RAKEs are completely overwhelmed by the strong interferer and give BER near one half. The LMS algorithm for MMSE is also unable to deal with the strong interferer and gives only marginally better performance than the RAKEs. The RLS algorithm on the other hand is able to completely excise this interferer and achieves the same performance as the noninterferer case shown in Fig. 5. The parity interferer case of SIR = 0 dB is given in Fig. 8 and we see that now both the RLS and LMS algorithms reject the NB interferer. The same is true of the analytic MMSE and the infinite RAKE. The matched filter, 4 and 8 finger RAKEs show about a 3 dB penalty relative to the no interference case.

In Fig. 9, we see the gradual degradation in performance of the 8 finger RAKE as the SIR varies. Results for the matched filter and 4 finger RAKE are similar, with poorer BER. In Fig. 10, the infinite RAKE also exhibits gradual degradation with increasing SIR. This range of SIR fills the performance range from ideal to complete collapse. The RLS algorithms

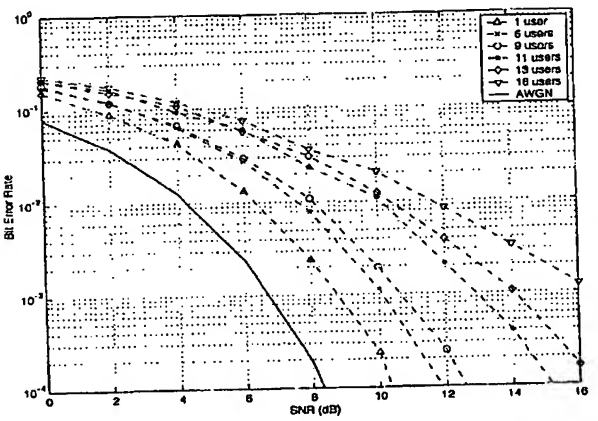

Fig. 16. BER performance of the MMSE using RLS algorithm with a sampling rate lower than Nyquist rate. The desired user's channel is fixed on a NLOS UWB channel [see Fig. 4(b)]. The number of UWB users varies from 1 to 16, where all users have the same received power.

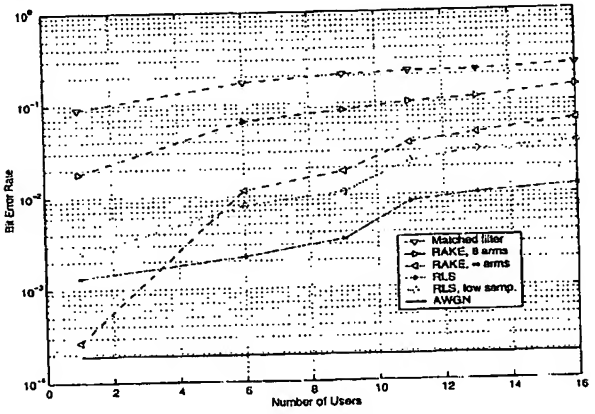

Fig. 17. BER performance versus number of users in the channel. The desired user's channel is fixed [see Fig. 4(b)] and SNR is fixed on 8 dB. The number of UWB users varies from 1 to 16, where all user(s) have the same received power.

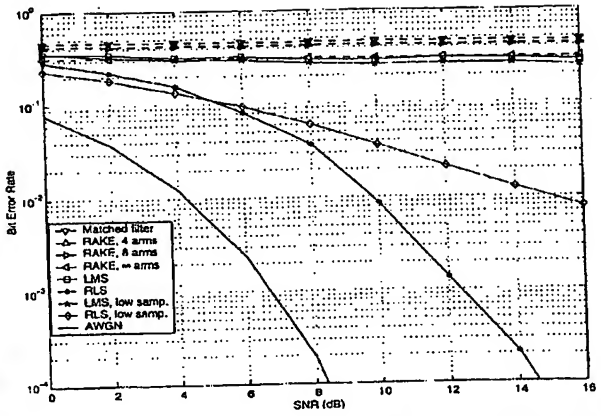

Fig. 18. BER performance in NLOS UWB channels in the presence of 15 UWB interferes all with the same received power and one OFDM interferer. SIR = −30 dB.

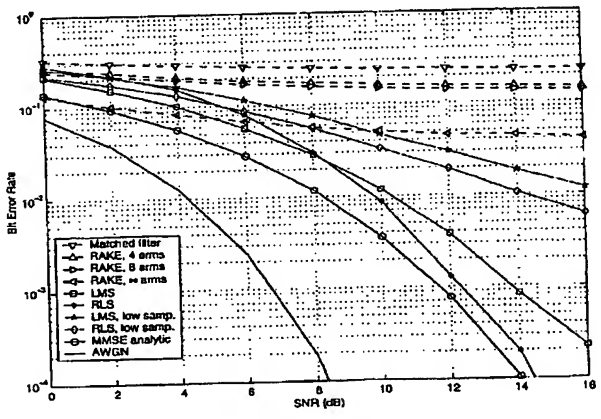

Fig. 19. BER performance in NLOS UWB channels in the presence of 15 UWB interferers and one OFDM interference. All UWB users have the same received power. SIR = 0 dB.

(both high and low sampling rates) have performance equal to the no interference case for the entire range of SIR, as seen in Fig. 11. The degradation of the LMS algorithm seen in Fig. 12 is not at all gradual as with the RAKEs. The LMS algorithm begins effectively rejecting the interferer from about −25 dB. Note that differences between the MMSE analytic results and simulated are due to insufficient training as the channel is static.

C. Multipath Channel, Multiple DS-CDMA UWB Signals

Results for this section are presented in Figs. 13–17, where we have averaged over 50 UWB channels in each case. The case of 15 asynchronous interfering signals is an extremely heavy load for a DS-CDMA system with length 15 spreading. In Fig. 13, we see that all RAKE receivers are overcome by the multiple access interference (MAI). Even the infinite RAKE exhibits flat BER of about 10%. The analytical results for the MMSE show about a 4-dB penalty while increasing the system throughput dramatically due to simultaneous transmissions. The high sampling rate RLS algorithm is able to capitalize on this MAI rejection capability, achieving the analytical bounds in high SNR region. The low sampling rate RLS shows a 6-dB penalty relative to the single user case (Fig. 5), but shows no error floor.

In Fig. 14, we see how the infinite RAKEs performance breaks down dramatically as more users are added to the system. With a reasonable load of five interferers, a 4-dB penalty is seen at BER $= 10^{-2}$ and 9-dB penalty by BER $= 10^{-3}$. The high sampling rate RLS in Fig. 15 shows only at most 3-dB degradation, and in Fig. 16 the low sampling rate RLS shows gradual degradation in performance as the number of interferers increases, to the maximum penalty of about 7 dB for the SNR values plotted. In Fig. 17, we fix the SNR to 8 dB, and

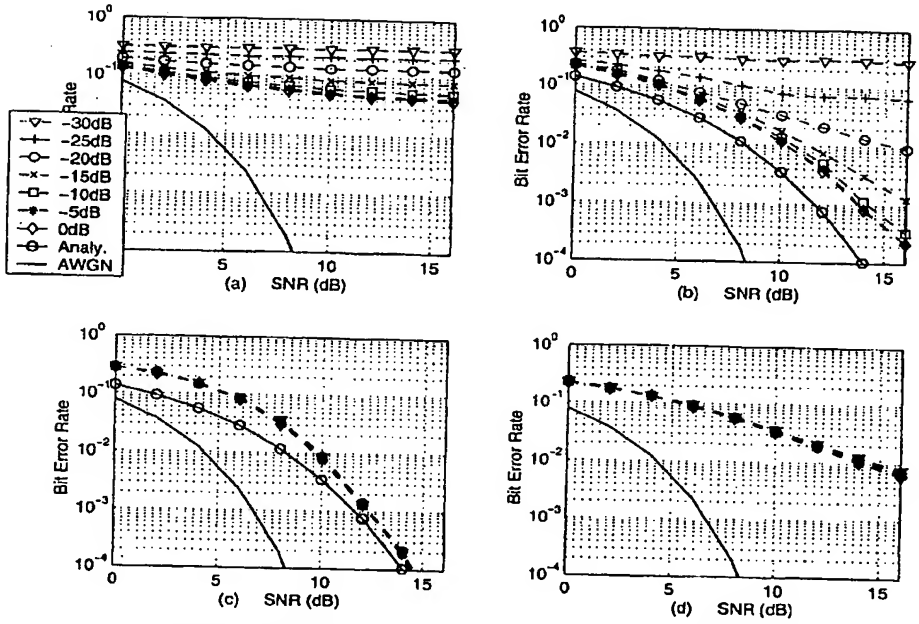

Fig. 20. The BER performance of four types for receiver in 16-user NLOS UWB channel with OFDM interference. SIR varies from −30 to 0 dB. (a) RAKE receiver with infinite number of fingers. (b) MMSE receiver using LMS algorithm. (c) MMSE receiver using RLS algorithm. (d) MMSE receiver using RLS algorithm and a sampling rate lower than the Nyquist rate of UWB signal.

plot the performance of various receivers versus the number of users in the system.

D. Multipath Channel, One NB Interferer and Multiple UWB Signals

Results for this section are presented in Figs. 18–20, where we have averaged over 20 UWB sets of channels in each case. For the extreme case of heavy network load (15 interferers) and strong narrowband interference, the performance of each receiver is plotted in Fig. 18. Only the high sampling rate RLS has reasonable performance—effectively rejecting the NB interferer, with only a 2-dB penalty compared with only wideband interferers. The low sampling rate RLS also continues to be effective against the NB interferer with a 4 dB penalty. All RAKE receivers have BER of one half, including the infinite RAKE.

In Fig. 19, we have a heavy MAI load, but SIR is now 0 dB. The previous performance (separate cases of MAI only and NB interference only) combine intuitively in this plot. The LMS and RLS are now able to reject the NB interference and are only limited by the MAI. The RAKE receivers have the same flat performance in Fig. 13 as the MAI dominates the NB interference.

Finally, in Fig. 20 we sweep through the values of the SIR while holding the MAI high at 15 interferers. We examine the performance of the of the infinite RAKE in (a), the LMS MMSE receiver in (b), the high sampling rate RLS MMSE receiver in (c), and the low sampling rate RLS MMSE receiver in (d). The RLS receivers reject all the NB interference, i.e., for all SIR. The LMS becomes effective at SIR = −20 dB, no longer exhibiting an error floor, while the infinite RAKE has flat performance for all SIR.

V. Conclusion

We have demonstrated the effectiveness of multiuser detection for a UWB pulse based direct sequence spread spectrum system using CDMA. Extensive simulations were run using channel soundings of the 2–8 GHz band collected in a residential setting. We examined the MMSE MUD detector ability to gather multipath energy and reject intersymbol and interchip interference for these channels. Despite extremely fragmented multipath for the NLOS channels, the ideal MMSE was able to achieve BER at only a 1 or 2-dB penalty from the AWGN lower bound. The adaptive MMSE showed only an additional decibel of loss over the ideal version. The RAKE receivers with four and eight arms were much less effective at gathering up the multipath energy (no interference present).

We examined the interference resistance of the MMSE MUD detector to a heavy load of multiple access interference (up to 16 users in a system with spreading length 15) and in the presence of a strong NB interferer following the IEEE 802.11a OFDM standard. The high sampling rate MMSE and the ideal MMSE were found to reject the NB interferer without problem even for SIR as severe as −30 dB. These idealized receivers also showed only a 4-dB penalty for the heavy MAI load versus the single user case. A more practical lower sampling rate adaptive MMSE receiver was also investigated (3 GHz sampling rate for

bit rates of 100 Mb/s and length 15 spreading code). This receiver also rejected the NB interferer handily and showed a 6-dB penalty for the heaviest load MAI investigated. The practical RAKE receivers were incapable of effectively rejecting either the strong narrowband interference or the heavily loaded wideband interference. Even more moderate levels of interference caused significant degradation in the performance of the practical RAKE receivers.

APPENDIX

Parameters: N_w = number of taps
j_0 = window starting point
Filter received signal using band pass filter and sample the filtered signal to
obtain digital samples $\tilde{r}(j), j = 1, 2, \ldots$.
Initialization: $\mathbf{w} = 0$.
Training Stage:
FOR $i = 1$: no. of training bits, **DO**
1) Get bandpass filtered data,
$\mathbf{u}(i) = [\tilde{r}(j_0 + (i-1)N_b + 1) \cdots \tilde{r}(j_0 + (i-1)N_b + N_w)]^T$;
2) Compute filter output,
$\beta(i) = \mathbf{w}^H \mathbf{u}(i)$;
3) Compute error,
$e = b_1(i) - \beta(i)$;
4) Update filter w based on LMS or RLS algorithm;
END
Decision-Direct Stage:
FOR i = no. of training bit + 1 : no. of bit in each packet, **DO**
1) Get bandpass filtered data,
$\mathbf{u}(i) = [\tilde{r}(j_0 + (i-1)N_b + 1) \cdots \tilde{r}(j_0 + (i-1)N_b + N_w)]^T$;
2) Compute filter output,
$\beta(i) = \mathbf{w}^H \mathbf{u}(i)$;
3) Estimate data bit,
$\hat{b}_1(i) = \text{sign}(\beta(i))$;
4) Compute error,
$e = \hat{b}_1(i) - \beta(i)$;
5) Update filter w based on LMS or RLS algorithm;
END

REFERENCES

[1] M. Z. Win and R. A. Scholtz, "Ultra-wide bandwidth time-hopping spread-spectrum impulse radio for wireless multiple-access communications," *IEEE Trans. Commun.*, vol. 48, pp. 679–691, Apr. 2000.

[2] U. Madhow, "Blind adaptive interference suppression for direct-sequence CDMA," *Proc. IEEE*, vol. 86, pp. 2049–2069, Oct. 1998.

[3] H. Fathallah and L. A. Rusch, "A subspace approach to adaptive narrowband interference suppression in DSSS," *IEEE Trans. Commun.*, vol. 45, pp. 1575–1585, Dec. 1997.

[4] S. Verdu, *Multiuser Detection*. Cambridge, U.K.: Cambridge Univ. Press, 1998.

[5] L. A. Rusch. (2001, Aug.) Indoor wireless communications: Capacity and coexistence on the unlicensed bands. *Intel Technical Journal* [Online]. Available: http://developer.intel.com/technology/itj/q32001/

[6] F. Ramirez-Mireles, "On the performance of ultra-wide-band signals in gaussian noise and dense multipath," *IEEE Trans. Veh. Technol.*, vol. 50, pp. 244–249, Jan. 2001.

[7] S. Haykin, *Adaptive Filter Theory*. Englewood Cliffs, NJ: Prentice-Hall, 1996.

[8] H. V. Poor and S. Verdu, "Probability of error in MMSE multiuser detection," *IEEE Trans. Inform. Theory*, vol. 43, pp. 858–871, May 1997.

[9] R. Durrett, *Probability: Theory and Examples*. Belmont, CA: Duxbury Press, 1995.

[10] L. A. Rusch, C. Prettie, D. Cheung, Q. Li, and M. Ho, Characterization of UWB propagation from 2 to 8 GHz in a residential environment, in *IEEE J. Select. Areas Commun.*, submitted for publication.

[11] J. G. Proakis, *Digital Communications*. Boston, MA: McGraw-Hill, 2000.

Qinghua Li (S'00–M'01) was born in Guangzhou, China, in 1970. He received the M.E. degree from Tsinghua University, Beijing, China, in 1995 and the Ph.D. degree from Texas A&M University, College Station, in 2001.

From 1995 to 1996, he was with Guangdong Telecommunication Academy of Science and Technology, China, and was involved in the development of telephone exchange networks. From 1996 to 2001, he was a Research Assistant in the Wireless Communications Laboratory, Texas A&M University, doing research in CDMA, turbo coding, and CMOS RF circuit design. In the summer of 2000, he worked as an Intern in Nokia Americas, Irving, TX, developing simulation tools for HDR CDMA. Since February 2001, he has been with the wireless research group of Intel Labs., Intel Corporation, Santa Clara, CA. His research interests are in the area of smart antenna network, ultra-wideband communications, multiuser detection, CDMA communications, and media access control protocols.

Leslie A. Rusch (S'91–M'94–SM'00) was born in Chicago, IL. She received the B.S.E.E. degree from the California Institute of Technology, Pasadena, in 1980 and the M.A. and Ph.D. degrees in electrical engineering from Princeton University, Princeton, NJ, in 1992 and 1994, respectively.

She is currently an Associate Professor in the Department of Electrical and Computer Engineering at Laval University, QC, Canada, and a member of COPL (Center for Optics, Photonics and Lasers). From 2000 to 2001, she was a Senior Staff Researcher at Intel Labs, Santa Clara, CA. Her research interests include fiber optic communications, spread-spectrum communications, CDMA for radio and optical frequencies, and ultra-wideband technology.